Bioorganic & Medicinal Chemistry 18 (2010) 8365–8373

Contents lists available at ScienceDirect

Bioorganic & Medicinal Chemistry

journal homepage: www.elsevier.com/locate/bmc

Design, synthesis and inhibition activity of novel cyclic peptides against protein tyrosine phosphatase A from *Mycobacterium tuberculosis*

Koushik Chandra, Debajyoti Dutta, Amit K. Das *, Amit Basak *

Department of Chemistry, Department of Biotechnology, Indian Institute of Technology, Kharagpur 721 302, India

ARTICLE INFO

Article history:
Received 13 July 2010
Revised 21 September 2010
Accepted 22 September 2010
Available online 7 October 2010

Keywords:
Peptide
Mycobacterium
Inhibition
Phosphatase
Tuberculosis

ABSTRACT

Mycobacterium tuberculosis, the causative agent for tuberculosis has employed several signalling molecules to sense the host cellular environment and act accordingly. For example, protein tyrosine phosphatase A (MPtpA) of *M. tuberculosis*, a signalling protein belonging to the tyrosine phosphatase superfamily, is involved in phagocytosis and is active in virulent mycobacterial form. Starting from a β-lactam framework a new class of structure based cyclic peptide (CP) inhibitors was designed. The synthesis involves a crucial intramolecular transamidation via a ring opening reaction. All the compounds show moderate to good inhibitory activities against MPtpA in micromolar concentrations. The results of inhibition kinetics suggest mixed mode of inhibition. The binding constant determined from circular dichroism (CD) and fluorescence quenching studies shows strong binding of the hydrophilic side chain of CPs with the enzyme active site residues. All these are well supported by docking studies.

1. Introduction

Protein phosphorylation and dephosphorylation are two important processes that are pivotal for the sustenance of the biological systems.[1] They have been identified as the key mediators of cell signalling and are required for cell division, control of metabolic activity, environmental response and pathogenicity. Understanding the role of these in enzymes and controlling their activities have been the focus of a rapidly growing research in the area of medicinal chemistry. Several pathogenic bacteria produce phosphatases which have been implicated to their virulence. One such example[2] is *Mycobacterium tuberculosis* which is the causative agent for tuberculosis (TB) and is a major cause of mortality throughout the world. Analysis of *M. tuberculosis* genome revealed the presence of MPtpA and MPtpB genes encoding protein tyrosine phosphatases MPtpA and MPtpB.[3] The bacillus releases MPtpA during its infection to macrophages and turns down the phagocytosis process.[4] Though the exact mechanism of its action is still unknown, the MPtps are now identified as potential targets for development of anti-tuberculosis agents and development of inhibitors of these enzymes is believed to be one of the ways to tackle the menace of TB. In this paper, we describe the synthesis of a series of novel cyclic peptides (CP). Their inhibitory activity against MPtpA have been evaluated and studied by different techniques and the results are also included.

The crystal structure of MPtpA[5] shows a PTP loop as a signature motif and the presence of Cys11, Arg17 and Asp126 as a part of the active site (Fig. 1). Its mechanism of action[1,6] as shown in Scheme 1 involves the nucleophilic attack by cysteine thiol followed by hydrolysis of the resulting thioacyl intermediate. Based upon the all these aspects and also the reported[7] inhibitory activity of cyclodepsipeptides, we have designed a new class of β-amino based cyclic peptides (CPs) as depicted in Figure 2. The rationale for our design is the possibility of H-bond and hydrophobic interactions that may occur with the CPs. The synthesized CPs were classified into three types (**A**–**C**) depending upon the number of α-amino acids connecting the β-amino acid to form the cyclic net-

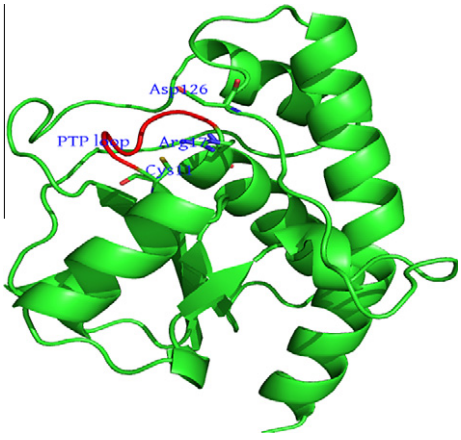

Figure 1. Cartoon structure of MPtpA showing the PTP loop (red) along with the active site residues Cys11, Arg17 and Asp126.

* Corresponding authors. Tel.: +91 3222 283300; fax: +91 3222 282252.
E-mail address: absk@chem.iitkgp.ernet.in (A. Basak).

0968-0896/$ - see front matter © 2010 Elsevier Ltd. All rights reserved.
doi:10.1016/j.bmc.2010.09.052

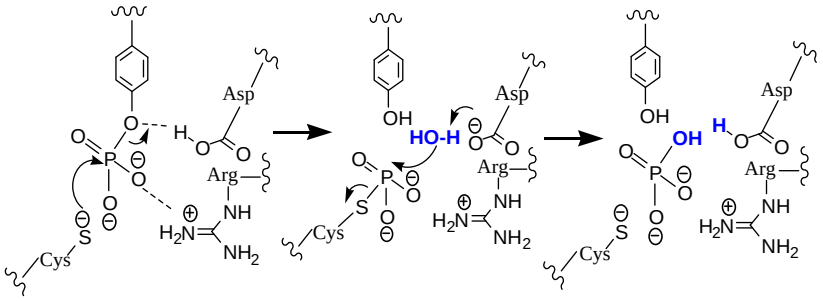

Scheme 1. The mechanism of the dephosphorylation catalysed by MptpA.

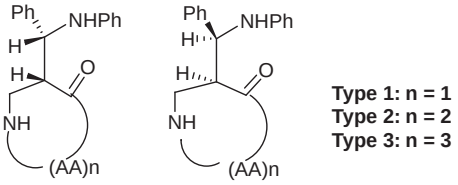

Figure 2. Prepared as a inseparable mixture of diastereomers.

work. These are shown in Figure 3 (for compounds **8**–**11**, please refer to Supplementary data).

2. Results and discussion

2.1. Synthesis

The various steps leading towards the synthesis of CPs are shown in Scheme 2. The key step is the intramolecular nucleophilic ring opening of a β-lactam with the free amine of an amino acid appendage. As a consequence, the β-amino acids were derived from the β-lactam skeleton itself. Thus in one step, we have been able to prepare the cyclic network along with the incorporation of the β-amino acid framework. The key intermediate, namely the cis 3-aminomethyl β-lactams (**16**–**17**)[8] (synthesized from the known hydroxyl-analogue via the Kinugasa reaction[9]) were coupled with *N*-Boc protected peptide to provide the β-lactam based acyclic peptides (**24**–**30**). These were deprotected with TFA and the salt was converted to the free amine by washing with sodium carbonate solution (**31**–**37**). Final transamidation step[10] involving intramolecular ring opening of β-lactam was carried out under different reaction conditions shown in Table 1. The table clearly shows that the cyclization becomes more facile in terms of yield and reaction time when acetic acid and triethyl amine were used as a buffer in EtOH. For higher member ring, the cyclization was even more facile possibly due to proper conformational alignment during cyclization.

All the compounds gave characteristic NMR and mass spectral data. The purity of the peptides was checked by hplc; however, in spite of all our attempts, the two diastereomers could not be separated, even by hplc. These were characterized as a mixture of two diastereomers (besides the ones reported here in the manuscript, four more CPs were synthesized and studied. The results are included in Supplementary data).

2.2. VT NMR study

Since H-bond interactions between the peptides and the enzyme should significantly contribute to their mutual binding, it is important to know the presence of any strong intramolecular H-bond, if any, in the CPs. Existence of any such interactions within the small molecules may rule out participation of the amide groups

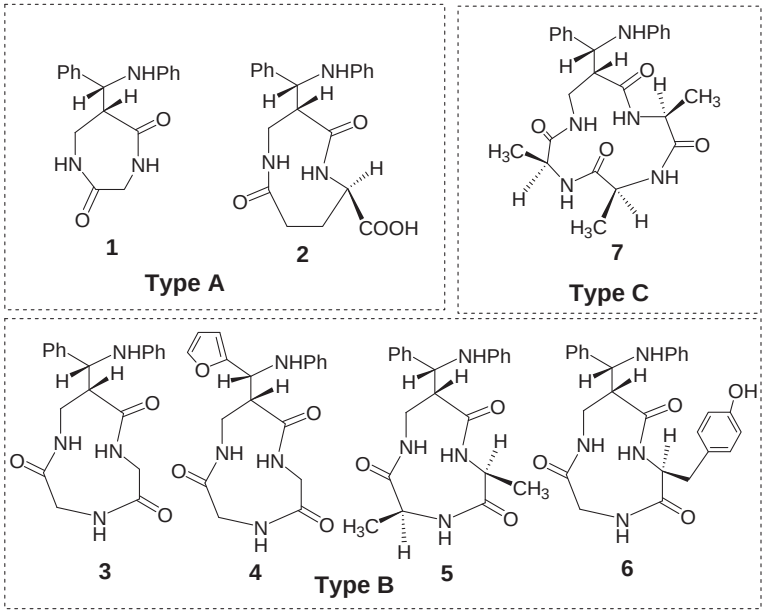

Figure 3. Synthesized cyclic peptides with different amino acid residues.

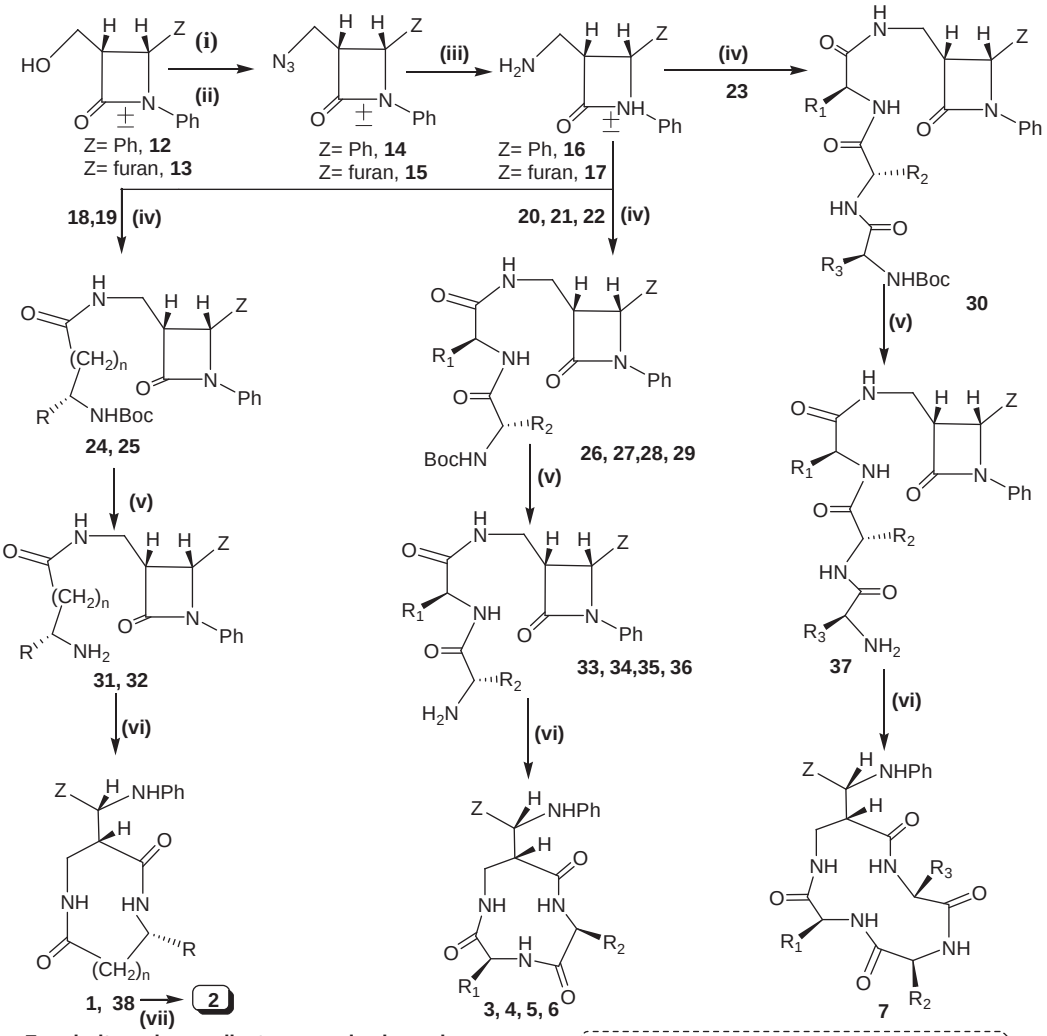

Scheme 2. Synthesis of Types 1, 2 and 3 CPs as diastereomeric mixture from cis β-lactam. Reagents and conditions: (i) MsCl, Et_3N, DCM, 0 °C, 10 min, 93–96%; (ii) NaN_3, dry DMF, rt, 3 h, 93–95%; (iii) PPh_3, moist THF, rt, overnight, 81–83%; (iv) EDC·HCl, HOBT, DIPEA, dry DCM/DMF, rt, 6 h, 75–78%; (v)TFA, dry DCM, 0 °C, then aqueous Na_2CO_3, 30 min, 69–72%; (vi) see Table 1, 65–70%; (vii) H_2, 10% Pd–charcoal, dry EtOH, rt, 85%.

Table 1
Reaction parameters for the intramolecular transamidation reaction for the synthesis of CPs

Entry	CPs (from amines)	Additives	Concn (M)	Temp (°C)	Reaction time (h)
1	**1–6**	None	2×10^{-2}	55	150
2	**7**	None	2×10^{-2}	50	95
3	**1–6**	0.5(M)Et_3N	2×10^{-2}	50	105
4	**7**	0.5(M)Et_3N	3×10^{-3}	50	55
5	**1**	0.5(M)Et_3N/0.05(M)AcOH	2×10^{-2}	45	38
6	**2–7**	0.5(M)Et_3N/0.05(M)AcOH	2.5×10^{-3}	45	25
7	**7**	0.5(M)Et_3N/0.05(M)AcOH	1.5×10^{-3}	45	18
8	**1–7**	1.0(M)Et_3N/0.5(M)AcOH	4×10^{-2}	60	88–110
9	**1–7**	1.1 mmol K_2CO_3	4×10^{-2}	60	72–120

in H-bonding interactions with the enzyme. In order to check that possibility, VT NMR was carried out with some of the peptides. The temperature coefficients ($\Delta\delta/\Delta T$)[11] of the various NHs were determined in $CDCl_3$ and are shown in Table 2.

Except for one NH of peptide **7**, which has a temperature coefficient of 3.1, there was no evidence of any strong intramolecular H-bonding meaning that the NHs and consequently the amide carbonyls are available for H-bonding with the enzyme residues (for plots of chemical shift vs temperature, see Supplementary data).

2.3. Inhibition study

Recombinant wild type MPtpA was purified as described previously.[12] Enzyme purity was assessed by SDS PAGE and protein concentration was determined from the absorbance at 280 nm. The phosphatase activity was measured at 25 °C using *p*-nitrophenol phosphate (*p*NPP) as substrate keeping a fixed concentration of protein (1 μM) in a reaction mixture of Tris buffer containing 0.1 M Tris, 0.15 M NaCl and 1 mM EDTA of pH 7.5. Synthetic CPs were dissolved in methanol and the methanol concentration was adjusted so as not to exceed 3% (v/v) in the final reaction mixture. This ensured the phosphatase activity of the enzyme to remain unaffected. The release of *p*-nitrophenol at 405 nm was quantified both in case of control and in presence of the inhibitors. The effective inhibitor and substrate concentrations were usually varied from 10–50 μm to 100–300 μm, respectively. Each assay was repeated in triplicate.

2.4. Data analysis

Using *p*NPP as a substrate, we have screened the CPs for possible inhibition of MPtpA activity. Values of the kinetic parameters and inhibitor constants were obtained from the Lineweaver–Burk plot (Fig. 4). For different concentration of same inhibitor, double reciprocal plots were taken into consideration to conclude the mode of inhibition. Inhibitory constant (K_i) was determined from the plot of $\left(\frac{K_m}{V_{max}}\right)$ vs [I] where [I] is the inhibitor concentration, K_m is the Michaelis–Menten constant and V_{max} is the maximum reaction velocity. All the compounds were found to behave as mixed inhibitors with K_i values in micromolar range (Table 3). Thus reversible binding interaction enabled the conformation change in PTP loop of MPtpA which in turn reflects in the rate of inhibition. However, such conformational irregularity became more pronounced in case of polar CPs bearing tyrosine or glutamic acid subunit compared to that observed for hydrophobic analogues. The tyrosine-based CP exerted maxima perturbation on MPtpA. However, the trans analogues of CPs were found to be comparatively less effective in inhibiting MPtpA.

2.5. CD measurement

CD measurement was accomplished on a Jasco-810 automatic recording spectropolarimeter using a quartz cell of path length 10 mm with the sample temperature maintained at 25 °C. The spectra were recorded in the range of 195–240 nm with a scan rate of 50 nm/min with a response period of 4 s. The spectra for MPtpA–CP **6** complex in far UV were obtained by subtracting the corresponding buffer blank containing CP **6** from the respective samples. CD spectra for each MPtpA–ligand complex were recorded by varying the concentration ratio up to 1:6. Finally the secondary structure was determined using CONTINLL of DICHROWEB,[13] an online server for protein secondary structure analysis from CD spectroscopic data.

Table 2
Amide proton NMR chemical shift temperature dependence in $CDCl_3$ (1 mM)

Peptides	Ring size	Amide-NH (**1**) ($-\Delta\delta_{NH}/\Delta T$) (ppb/K)	Amide-NH (**2**) ($-\Delta\delta_{NH}/\Delta T$) (ppb/K)	Amide-NH (**3**) ($-\Delta\delta_{NH}/\Delta T$) (ppb/K)
1	7	6.4	6.7	—
4	10	9.2	6.1	—
6	10	10.5	5.6	—
7	13	**3.1**	5.5	5.8

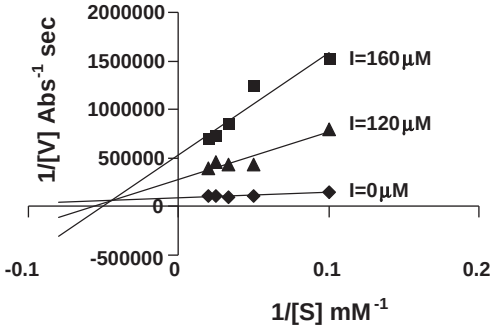

Figure 4. Lineweaver–Burk plot for CP **6**.

Table 3
Inhibitory constants (K_i) of CPs

Compound	K_i (μM)
1	140.2 ± 10
2	36.3 ± 8.5
3	85.5 ± 7.3
4	215.4 ± 12
5	220.2 ± 11
6	8.0 ± .20
7	199.1 ± 10

2.6. Determination of binding constant from CD data

Changes in structural properties of MPtpA caused by the binding of above synthesized CPs are essential in understanding the mechanism of action and regulation of biological activity. For this it is important to observe any change in the secondary structural motif like α-helix of MPtpA which appears as negative bands in the far UV-region with the minima at 208 nm and 222 nm. The CPs alone in Tris buffer did not exhibit any significant peaks in these particular regions. Then we performed the titration based kinetics studies between CPs and MPtpA in such a way that the concentration ratio was varied upto 6:1 (one representative CD-titration curve for compound **6** is shown in Figure 5; for others, please refer to Supplementary data).

It was found that the regions characteristic of the α-helix were affected due to gradual increase in concentration of all cyclic peptides which substantiates the unfolding of the protein. Such conformational changes were even more pronounced in case of those CP, which contain polar components like carboxylic acid or phenolic-OH group etc. These findings clearly suggest that these CP have the tendency to interact strongly with the α-helix associated with PTP loop in MPtpA by virtue of complementary binding sites.[14] The red shift of the band in CD spectra also indicates the formation of stable transition state complex. A similar phenomenon was observed when we performed the time dependent CD spectroscopy between MPtpA and compound **6** (Table 4). As the time proceeds, the disruption of α-helix takes place ending up in a random coil conformation.

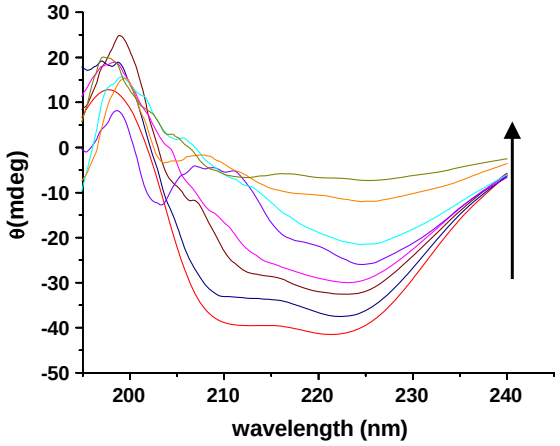

Figure 5. Overlayed deconvoluted CD spectra recorded during complexation between MptpA and different concentration of CP-**6**. Upward arrow shows the gradual increase in concentration ratio (MPtpA/CP-**6**) (i) only MPtpA; (ii) 2:1; (iii) 1:1; (iv) 1:2; (v) 1:3; (vi) 1:4; (vii) 1:5; (viii) 1:6.

Table 4
Changes in secondary structure of MPtpA. Upon interaction with CP-**6** at different time interval

Time (min)	Helix (%)	Strands (%)	Turns (%)	Unordered (%)
0	42	8.9	16.8	32.2
5	41.5	12	20.9	25.5
10	36.1	15.2	15.2	33.5
15	28.9	27.7	17.9	25.3
20	22.7	27.3	19.1	30.9
30	16.3	39.2	21.4	23.0
45	12.3	37.3	13.9	36.5
60	2.1	25.0	18.3	56.5
90	0.9	31.5	17.7	46.8
180	0	16.9	38.7	43.7

We have also calculated the binding constants (Table 5) of the CPs upon complexation with the protein by direct titration method. For such interaction it is assumed that there is only 1:1 complex formation in which the MPtpA. CP complex is in equilibrium with unreacted free MPtpA and CP, that is, ([MPtpA] + [CP] = [MPtpA. CP]. The equation used for the calculation is $1/[\theta] = 1/[\theta]_{max} + 1/[\theta]_{max}K_bC_P$ in which C_P represents the initial concentration of CP, [θ] is the difference in absorption in presence and in absence of inhibitor and K_b is the binding constant between MPtpA and CPs. The double reciprocal plot of $1/[\theta]$ versus $1/C_P$ is linear and the binding constant (K_b) is obtained by taking the ratio of intercept to the slope. The higher the binding constant, the greater is the perturbation. From the binding constant values (Table 5) it is again the tyrosine and glutamic acid-based inhibitors that exerted relatively greater extent of perturbation on α-helix as compared to other non-polar hydrophobic analogues.

Table 5
Binding constant of CPs from CD

CPs	K_b (M^{-1}) at 222 nm
1	3.6×10^4
2	8.5×10^4
3	4.7×10^4
4	2.95×10^4
5	1.1×10^4
6	1.2×10^5
7	3.3×10^4

2.7. Fluorescence studies

Intrinsic tryptophan fluorescence of native and chemically denatured samples were monitored by Hitachi spectrofluorometer using a quartz cuvette of 10 mm path length at a fixed temperature of 20 °C, equipped with a constant temperature water circulator bath (NesLab). Baseline correction was made by subtracting the spectra of CP from respective measurements. The protein was excited at 295 nm and the emission spectra were recorded starting from 305 nm to 550 nm with emission maxima at 340 nm. Multiple scans were taken in each case. The spectrum of MPtpA shows maxima at 340 nm indicating the presence of tryptophan residue. There was a quenching of fluorescence in presence of the inhibitor and the interactions were explained in terms of Stern–Volmer equation[15] and Scatchered plot.[16]

2.8. Steady state fluorescence quenching

The origin of intrinsic fluorescence of MPtpA is guided by the presence of aromatic amino acid tryptophan where the indole moiety is responsible for UV absorbance and the fluorescence of the protein. Henceforth it provides a fundamental tool to extract information about the mode of interaction of MPtpA. Based on this approach, fluorometric titration of MPtpA and CP were performed by varying the concentration from 2.5 μM to 20 μM. The intensity maximum at 340 nm was found to diminish gradually with increasing concentration of CP. One representative fluorescence-titration curve for compound **6** is shown in Figure 6 (for others, refer to Supplementary data). The quenching phenomenon was well observed up to the concentration ratio 1:10. This offers a valuable explanation that CP interacts with the PTP loop in such a way that two tryptophan residues simultaneously get buried leading to fluorescence quenching. In addition, the polar subunits like carboxylic acid or phenolic-OH interact even strongly resulting in a greater extent of quenching behaviour. The induction of polar residues to CP not only brought about the conformational change of MPtpA but it also throws light to the probable route of the interaction process. The time dependent interaction studies between CP and MPtpA also reflected the similar behaviour. Finally, the binding constants have been calculated for each complex by direct titration method.

The quenching of fluorescence was analyzed (Fig. 7) following the classical Stern–Volmer equation. $F_0/F = 1 + K_{sv}[Q]$ where the F_0 and F are the fluorescence intensity in absence and in presence of a quencher, [Q] is the molar concentration of quencher and K_{sv} is the collision quenching constant [M^{-1}]. The MPtpA concentration was kept 2 μM throughout the experiment. Binding constant was

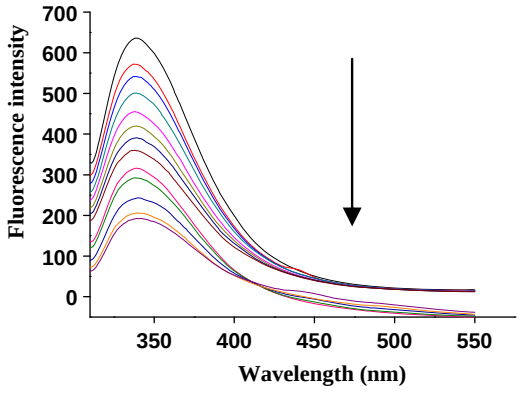

Figure 6. Overlayed deconvulated fluorescence spectra of the complexation between MptpA and different concentration of CP-**6**. Downward arrow shows the quenching.

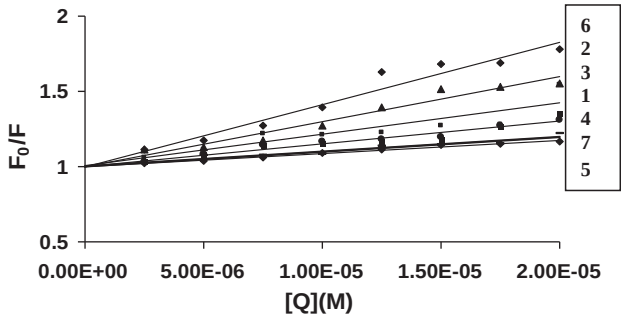

Figure 7. Overlayed deconvulated Stern–Volmer plots.

determined from the equation, $\log (F_0 - F)/F = \log K_b + n \log [Q]$, where K_b is the binding constant and n is the number of binding site. The binding constants as shown in Table 6, are high for tyrosine and glutamic acid-based CP which substantiates the fact that hydrophilic together with π-stacking interactions play a dominant role upon complexation with MPtpA. All the interactions support 1:1 binding indicating that the inhibitor binds to a specific site of MPtpA.

2.9. Docking materials

Coordinates of MPtpA were retrieved from Protein Data Bank (PDB ID 1U2P). Docking was performed using Dock6[17] in association with Chimera[18] visualization interface. Accessible surface was calculated using PISA server (http://www.ebi.ac.uk/msd-srv/prot_int/pistart.html). Protein model illustration with bound inhibitor was carried out using Pymol (http://www.pymol.sourceforge.net). The goal of the docking studies was to substantiate the facts related to the conformational aspects of preferred binding with MPtpA and the molecular mechanism of its inhibitory effect on MPtpA.

2.10. Docking study

In MPtpA, the PTP loop functions as the key element for its flexible accessibility of the substrate to the active site and also directing the catalytic mechanism pivotal for various types of interaction with different substances. The loop undergoes a large conformational change housing two active site residues Cys11 and Arg17. Therefore, the ligand induced flexibility of the PTP loop is important to exert catalysis via an optimized interaction with polar residues. The important substitution in PTP loop of *M. tuberculosis* is Leu12 instead of Thr present in mammalian PTP loop.

As inferred from the docking studies that although most of the CPs are effective in recognizing the active site and its surroundings, their effectiveness depends on their ring substitutions. The mode of the binding depends on the relative perturbation of the interacting residues. Apart from the active site residues, Glu125, Trp48, Thr12 are also able to strengthen the binding of the CP. Among all, tyrosine-based CP **6** which exhibited the highest inhibition, was found to have greater impact on secondary structure of MPtpA in terms of availability of the maximum number of hydrogen bonding as well as suitable hydrophobic and π-stacking interaction shown in Table 7. The probable interactions of CP **6** with different residues of MPtpA are shown in Figure 8. The cyclic peptide backbone is stabilized by the hydrogen binding interaction with Arg17 and Thr12 located at the two ends of the PTP loop. Perturbation of the PTP loop associated α-helix is already confirmed by CD experiments. The stacking interaction of *N*-Phenyl group in **CP 6** with Tyr128 and the van der Wall interaction with Trp48 are also notable. Interaction between Trp48 and CP **6** is also confirmed by the fluorescence quenching experiments. In addition, two aryl rings of CP **6** fit into the hydrophobic groove of MPtpA causing restricted movement of PTP loop.

Thus comparative docking analysis was able to throw light on the nature of interaction of the CPs with the protein and was also in agreement with other physical measurements.

Table 6
Binding constant of CPs from fluorescence

Compound	K_b (M^{-1}) at 295 nm
1	3.41×10^4
2	8.89×10^4
3	4.87×10^4
4	2.99×10^4
5	1.0×10^4
6	1.5×10^5
7	3.27×10^4

2.11. Conclusion

A new class of CPs has been identified as a potential candidate for MPtpA inhibitor. Three types depending on the number of amino acids of CPs were synthesized from β-lactam intermediates via novel intramolecular transamidation reaction. These CPs constitute a core where a common residue β-alanine is attached to various polar and non-polar amino acids. The functional groups in polar and non-polar residues impart a significant contribution towards the complexation with target MPtpA. VT NMR reveals the absence of strong intramolecular H-bond except for compound **11** which showed strong intramolecular H-bond for one of the NHs. Therefore with the presence of sufficient number of hydrogen bonding locations available for the interaction with enzyme, all CPs interacted strongly with MPtpA as reflected in their K_i values. Although the exact mode of interaction by possible X-ray structure of co-crystal is currently under investigation, CD studies and fluorescence quenching of tryptophan residues predicted significant perturbation of helix structure. Docking experiments suggest that all the CPs bind strongly to the PTP loops of the signature motif which influences the associated helix and hydrophobic tryptophan residue to a greater extent. However, small modification to the chemical structure generates profound alterations in the mode of interaction to the target enzyme. While the tyrosine-based CP showed much impact on the phosphorylation state of the target enzyme, their trans analogues have little influence on the enzyme as evident from kinetics of inhibition, CD and fluorescence study. Further studies are on the way to bring down the inhibition to nanomolar range by suitable changes in the structure of CPs.

3. Experimental

All ^{1}H NMR and ^{13}C NMR spectra were recorded in $CDCl_3$ at 400 MHz unless otherwise mentioned. IR was recorded using Thermo Nicolet FT-IR. Mass spectra were analyzed by Waters LCT mass spectrometer. Enzyme purity was assessed by SDS–PAGE and protein concentration was determined from the absorbance at 280 nm. 0.1 M Tris–HCl pH 7.5 having ionic strength 0.15 M of NaCl and 1 mM EDTA was used for the kinetic study with all the synthesized compounds. CD and fluorescence measurement were recorded on Jasco-810 automatic recording spectropolarimeter and Hitachi spectrofluorometer respectively using a quartz cell of path length 10 mm.

3.1. General procedure for the synthesis of β-lactam linear peptides conjugates

To a solution of *N*-Boc protected free acid of linear peptide (1 equiv) in 2:1 DCM/DMF mixture (10 mL/5 mL), 1-[3-dimethyl aminopropyl]-3 ethyl carbodiimide hydrochloride (EDC·HCl)

Table 7
Docking interaction analysis during complexation between MPtpA and CP **6**

Interacting protein residues (atom)	Interacting counterpart of CP **6**	Interaction distance (Å)	Remarks
Thr12 (OG1)	Amide oxygen	3.2	Present in PTP loop (H-bonding)
Arg17 (NH2)	Amide oxygen	2.9	Located at C-terminal part of the PTP loop (H-bonding)
Tyr128	NHPh group	4.2	Aromatic π-stacking interaction
Glu125 (OE1)	Tyrosine oxygen	3.9	Polar interaction
Trp48	Two outer Ph-rings	4.7	Hydrophobic interaction
Asp126 (OD2)	Amide nitrogen	3.9	Polar interaction

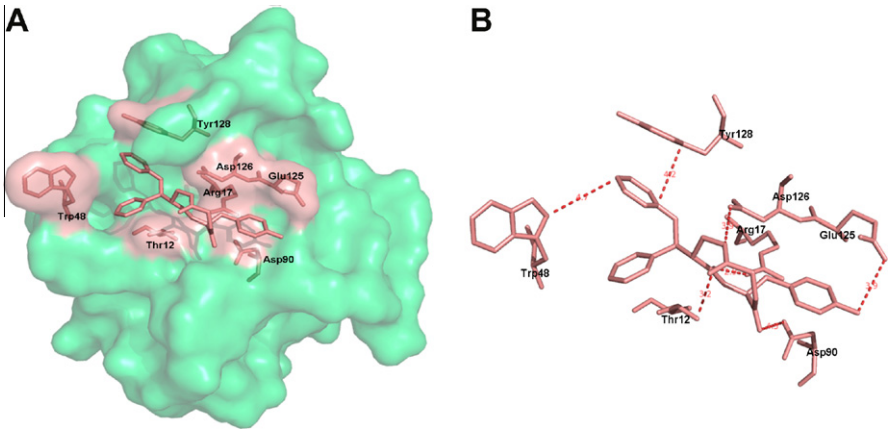

Figure 8. CP **6** docked on MPtpA. (A) CP **6** sits in the cleft near the active site. Interacting residues are shown in salmon colour. Thr12 and Arg17 are part of the PTP–loop. (B) Different interactions between the MPtpA residues with CP **6** are shown.

(1.2 equiv) followed by 1-hydroxy benztriazole (HOBT) (1.2 equiv) were stirred at 0 °C for 15 min. The β-lactam containing free amine (1 equiv) were added dropwise at 0 °C followed by diisopropyl ethyl amine (DIPEA) (3 equiv). The whole mixture was left stirring for overnight at room temperature. After partitioning between DCM and water, the organic layer was washed first with aq $NaHCO_3$, dil HCl, brine and finally dried over sodium sulfate and evaporated. The oily crude mixture was purified by column chromatography (60–120 silica gel) using 2:1 hexane/EtOAC mixture.

3.1.1. {[(2-Oxo-1,4-diphenyl-azetidin-3-ylmethyl)-carbamoyl]-methyl}-carbamic acid *tert*-butyl ester (24)

Yield 78%; off-white solid; γ_{max} (KBr/cm^{-1}) 1645, 1743, 2372, 3436; δ_H 1.45 (9H, s), 3.16–3.27 (2H, m), 3.70–3.73 (2H, m), 3.83 (1H, q, J = 7.2 Hz), 5.25 (1H, d, J = 6.0 Hz), 5.32 (1H, br s), 6.41 (1H, br s), 7.04–7.08 (1H, m), 7.22–7.39 (9H, m); δ_C 28.3, 31.6, 36.0, 52.8, 57.0, 80.4, 117.1, 124.2, 126.7, 128.7, 129.1, 134.0, 137.2, 156.5, 165.8, 169.3; HRMS calcd for $C_{23}H_{27}N_3O_4 + H^+$ 410.2080 found 410.2084.

3.1.2. 2-*tert*-Butoxycarbonylamino-4-[(2-oxo-1, 4-diphenyl-azetidin-3-ylmethyl)-carbamoyl]-butyric acid (25)

Yield 77%; off-white solid; isolated as inseparable mixture of diastereomers; γ_{max} (KBr/cm^{-1}) 1645, 1745, 2365, 3431; δ_H 1.44 (9H, s), 1.84–2.48 (6H, m), 3.26 (1H, m), 3.69–3.82 (1H, m), 4.03 (1H, br s), 4.29 (1H, br s), 5.10–5.25 (3H, m), 7.05–7.08 (1H, m), 7.26–7.45 (9H, m); δ_C [Major isomer] 27.9, 28.2, 35.9, 37.1, 51.7, 52.8, 57.0, 67.1, 80.2, 110.2, 116.7, 117.0, 124.0, 124.1, 125.8, 126.6, 128.4, 128.5, 128.6, 128.7, 128.9, 129.0, 129.1, 130.8, 133.9, 137.2, 143.5, 165.5, 165.7, 171.2, 171.2; [Minor isomer] 27.8, 28.8, 35.9, 38.6, 51.1, 52.9, 58.7, 68.0, 80.2, 110.8, 116.7, 117.0, 124.0, 124.1, 125.8, 126.6, 128.3, 128.5, 128.6, 128.7, 128.9, 129.0, 129.1, 130.8, 133.9, 137.2, 143.5, 165.5, 165.7, 171.2, 171.2; HRMS calcd for $C_{26}H_{31}N_3O_6 + H^+$ 482.2291 found 482.2293.

3.1.3. [({[(2-Oxo-1,4-diphenyl-azetidin-3-ylmethyl)-carbamoyl]-methyl}-carbamoyl)-methyl]-carbamic acid *tert*-butyl ester (26)

Yield 78%; off-white solid product; γ_{max} (KBr/cm^{-1}) 1642, 1750, 2373, 3435. δ_H 1.45 (9H, s), 3.06–3.12 (1H, m), 3.22–3.29 (1H, m), 3.80–3.94 (5H, m), 5.24 (1H, d, J = 5.6 Hz), 5.32 (1H, br s), 6.45 (1H, br s), 6.93 (1H, br s), 7.04–7.09 (1H, m), 7.22–7.39 (9H, m); δ_C 28.2, 36.1, 42.8, 44.4, 52.4, 57.0, 80.5, 117.1, 124.1, 125.8, 126.6, 128.7, 129.0, 133.8, 137.1, 165.7, 168.4, 169.9; HRMS calcd for $C_{25}H_{30}N_4O_5 + H^+$ 467.2294 found 467.2298.

3.1.4. [({[(2-Furan-2-yl-4-oxo-1-phenyl-azetidin-3-ylmethyl)-carbamoyl]-methyl}-carbamoyl)-methyl] carbamic acid *tert*-butyl ester (27)

Yield 74%; off-white solid; γ_{max} (KBr/cm^{-1}) 1643, 1749, 2370, 3427. δ_H 1.35 (9H, s), 3.40–3.55 (2H, m), 3.80–3.95 (5H, m), 5.22 (1H, d, J = 5.6 Hz), 5.31 (1H, br s), 6.39 (2H, m), 6.63 (1H, br s), 6.99 (1H, br s), 7.05–7.09 (1H, m), 7.24–7.27 (4H, m), 7.42 (1H, br s); δ_C 28.2, 31.5, 36.0, 42.9, 51.1, 53.0, 81.2, 110.4, 110.7, 116.8, 124.2, 124.9, 129.0, 131.1, 137.1, 143.5, 147.9, 165.6, 168.8, 170.1; HRMS calcd for $C_{23}H_{28}N_4O_6 + H^+$ 457.2087 found 457.2092.

3.1.5. (1-{1-[(2-Oxo-1,4-diphenyl-azetidin-3-ylmethyl)-carbamoyl]-ethylcarbamoyl}-ethyl)-carbamic acid *tert*-butyl ester (28)

Yield 76%; yellowish solid; isolated as inseparable mixture of diastereomers; γ_{max} (KBr/cm^{-1}) 1643, 1746, 2366, 3432; δ_H 1.25–1.31 (6H, m), 1.45 (9H, s, Boc), 3.06–3.29 (2H, m), 3.78–3.86 (1H, m), 4.14 (1H, m), 4.28–4.40 (1H, m), 5.26 (1H, d, J = 6.0 Hz), 6.25 (1H, br s), 6.35 (1H, br s), 6.70 (1H, br s), 7.04–7.08 (1H, m), 7.23–7.38 (9H, m); δ_C [Major isomer] 18.3, 18.3, 28.3, 31.5, 36.0, 48.8, 52.6, 57.0, 80.2, 117.1, 117.1, 124.0, 124.1, 126.7, 126.7, 126.8, 128.6, 129.0, 133.9, 134.0, 137.2, 165.7, 172.0, 172.3, 172.7; [Minor isomer] 18.3, 18.3, 28.3, 31.5, 36.2, 48.7, 52.8, 57.0, 80.2, 117.1, 117.1, 124.0, 124.1, 126.7, 126.7, 126.8, 128.6, 129.1,

133.9, 134.0, 137.2, 165.7, 172.1, 172.3, 172.7; HRMS calcd for $C_{27}H_{34}N_4O_5 + H^+$ 495.2607 found 495.2612.

3.1.6. [2-(4-Hydroxyphenyl)-1-({[(2-oxo-1,4-diphenyl-azetidin-3-ylmethyl)-carbamoyl]-methylcarbamoyl)-ethyl]-carbamic acid *tert*-butyl ester (29)

Yield 75%; white semi-solid; isolated as inseparable mixture of diastereomers; γ_{max} (KBr/cm^{-1}) 1628, 1749, 2375, 3630; δ_H 1.42 (9H, s), 2.87–3.15 (4H, m), 3.65–3.81 (3H, m), 4.50 (1H, m), 5.14 (1H, m,), 6.34 (1H, br s), 6.70–7.34 (14H, m); δ_C [Major isomer] 28.2, 35.9, 44.1, 52.6, 53.2, 54.2, 57.0, 80.2, 110.7, 115.6, 116.8, 117.1, 121.5, 121.7, 124.1, 126.6, 127.4, 128.6, 128.9, 129.0, 130.2, 130.3, 133.7, 133.8, 137.1, 143.5, 155.5, 166.0, 169.7, 171.0; [Minor isomer] 28.2, 37.2, 44.1, 53.0, 54.0, 54.3, 56.9, 80.2, 110.5, 115.6, 116.8, 117.1, 121.5, 121.7, 124.1, 126.6, 127.4, 128.6, 128.9, 129.0, 130.2, 130.3, 133.7, 137.0, 137.1, 143.5, 155.2, 165.9, 170.5, 170.9; HRMS calcd for $C_{32}H_{36}N_4O_6 + H^+$ 573.2713 found 573.2715.

3.1.7. [1-(1-{1-[(2-Oxo-1,4-diphenyl-azetidin-3-ylmethyl)-carbamoyl]-ethylcarbamoyl} ethyl carbamoyl) ethyl]-carbamic acid *tert*-butyl ester (30)

Yield 75%; yellowish semi-solid; isolated as inseparable mixture of diastereomer; γ_{max} (KBr/cm^{-1}) 1645, 1748, 2375, 3442; δ_H 1.25–1.47 (18H, m), 3.07–3.27 (2H, m), 3.94 (1H, m), 4.13–4.41 (3H, m), 5.08 (1H, br s), 5.26 (1H, dd, J = 5.6 Hz, J = 6.0 Hz), 6.51 (1H, br s), 6.94 (1H, br s), 7.03–7.08 (1H, m), 7.25–7.38 (9H, m); δ_C [Major isomer] 17.9, 18.1, 18.4, 28.3, 36.0, 48.9, 49.1, 51.4, 52.9, 57.4, 80.5, 117.1, 124.0, 124.1, 126.7, 126.9, 128.5, 128.6, 128.9, 129.1, 133.9, 134.0, 137.4, 156.1, 165.9, 172.1, 172.2, 173.8; [Minor isomer] 17.9, 18.1, 18.4, 28.3, 36.0, 49.1, 49.7, 51.2, 52.5, 57.2, 80.5, 117.1, 124.0, 124.1, 126.7, 126.9, 128.5, 128.6, 128.9, 129.1, 133.9, 134.0, 137.2, 156.1, 166.0, 172.0, 172.3, 173.1; HRMS calcd for $C_{25}H_{31}N_5O_4 + H^+$ 466.2454 found 466.2455.

3.2. General procedure for the deprotection of *N*-Boc β-lactam peptides conjugates

The *N*-Boc-protected β-lactam-peptides conjugates (1 equiv) dissolved in 10 ml dry DCM was treated dropwise with TFA (20 equiv) at 0 °C for 30 min. The mixture was evaporated in vacuo, washed twice with benzene and finally diluted with Na_2CO_3 solution followed by EtOAc. The solution was stirred for another 30 min. The organic layer was separated, washed with brine and dried over anhydrous sodium sulfate solution. Finally organic layer was concentrated in vacuo. The crude product obtained can be treated as pure solid starting material (R_f = 0.3, 5:1 DCM/MeOH) without being further purification by column chromatography.

3.3. General procedure for the synthesis of cyclic peptides

The β-lactam containing peptidyl free amine (1 equiv) was dissolved under high dilution condition in distiled EtOH (20 ml) in presence of a buffer mixture of Et_3N and acetic acid. The overall mixture was stirred at 40–60 °C for several hours as indicated in Table 1. After checking the TLC the reaction was quenched by adding saturated $NaHCO_3$ solution. It was washed with 1 N HCl followed by brine and finally extracted with EtOAc before drying over anhydrous sodium sulfate solution. The organic layer was concentrated in rotavapor and the crude mixture was then purified in flash chromatography (230–400 silica gel) using DCM/MeOH mixture (50:1–10:1) solvent (R_f = 0.3) yielding 65–73% non separable mixture of diastereomeric products. All the diastereomers has been well characterized by NMR and Mass spectrometry after further purified by HPLC.

3.3.1. 6-(Phenyl-phenylamino-methyl)-[1,4]diazepane-2,5-dione (1)

Yield 73%; yellowish semi-solid; γ_{max} (KBr/cm^{-1}) 1654, 1741, 2345, 3431; δ_H 3.14–3.28 (2H, m), 3.75–3.89 (3H, m), 5.25 (1H, d, J = 5.6 Hz), 6.12 (1H, br s), 6.28 (1H, br s), 7.05–7.09 (1H, m), 7.26–7.36 (9H, m); δ_C 36.0, 43.0, 52.6, 57.0, 117.1, 124.0, 124.2, 126.7, 127.0, 128.7, 128.8, 129.1, 129.1, 133.9, 134.3, 137.1, 168.9, 170.7; HRMS: calcd for $C_{18}H_{19}N_3O_2 + H^+$ 310.1556 found 310.1559.

3.3.2. 4,9-Dioxo-3-(phenyl-phenylamino-methyl)-[1,5]diazonane-6-carboxylic acid (2)

Yield 68%; yellowish powder; was obtained as an inseparable mixture of diastereomer; γ_{max} (KBr/cm^{-1}) 1631, 1755, 2336, 3670; δ_H 2.08–2.45 (4H, m), 2.95–3.29 (1H, m), 3.85 (1H, m), 4.03–4.11 (1H, m), 5.25 (1H, d, J = 4.8 Hz), 6.61 (1H, br s), 6.82 (1H, br s), 7.07 (1H, m), 7.23–7.44 (9H, m); δ_C: [Major isomer] 25.7, 29.1, 36.2, 52.3, 56.8, 57.0, 116.8, 117.1, 124.3, 125.8, 126.6, 128.7, 128.8, 129.1, 129.2, 133.8, 137.1, 143.7, 155.9, 167.6, 172.0; [Minor isomer] 25.7, 29.2, 36.2, 52.2, 56.8, 57.0, 116.8, 117.1, 124.3, 125.8, 126.6, 128.7, 128.8, 129.1, 129.2, 133.8, 137.1, 143.8, 154.0, 159.0, 166.3; HRMS calcd for $C_{21}H_{24}N_3O_4 + H^+$ 382.1767 found 382.1770.

3.3.3. 9-(Phenyl-phenylamino-methyl)-[1,4,7]triazecane-2,5,8-trione (3)

Yield 73%; off-white semi-solid; γ_{max} (KBr/cm^{-1}) 1654, 1741, 2369, 3432; δ_H 3.03 (1H, m), 3.27 (1H, m), 3.81–3.97 (5H, m), 5.25 (1H, d, J = 5.6 Hz), 6.51 (1H, br s), 6.95 (1H, br s), 7.08 (1H, m), 7.26–7.37 (9H, m); δ_C 36.2, 42.8, 43.4, 52.2, 57.0, 117.1, 124.2, 126.5, 128.7, 129.0, 129.1, 133.7, 137.0, 166.2, 168.5, 169.4; HRMS calcd for $C_{20}H_{22}N_4O_3 + H^+$ 367.1770 found 367.1776.

3.3.4. 9-(Furan-2-yl-phenylamino-methyl)-[1,4,7]triazecane-2,5,8-trione (4)

Yield 72%; off-white semi-solid; γ_{max} (KBr/cm^{-1}) 1645, 1751, 2368, 3410; δ_H 3.31–3.69 (7H, m), 4.65 (1H, br s), 5.22 (1H, d, J = 5.6 Hz), 6.40 (2H, m), 6.75 (1H, br s), 7.08 (1H, m), 7.26 (4H, m), 7.43 (1H, br s); δ_C 36.0, 44.4, 51.2, 52.9, 62.1, 110.4, 110.7, 116.8, 116.8, 124.4, 129.1, 137.1, 143.6, 143.6, 147.8, 167.7, 167.9, 169.8; HRMS calcd for $C_{18}H_{20}N_4O_4 + H^+$ 357.1563 found 357.1567.

3.3.5. 3,6-Dimethyl-9-(phenyl-phenylamino-methyl)-[1,4,7]-triazecane-2,5,8-trione (5)

Yield 70%; off-white semi-solid product which was isolated as inseparable mixture of diastereomer; γ_{max} (KBr/cm^{-1}) 1646, 1742, 2368, 3435; δ_H 1.25–1.46 (6H, m), 3.12–3.27 (2H, m), 3.45–3.50 (1H, m), 3.69–3.82 (2H, m), 5.24 (1H, m), 6.74 (1H, br s), 7.06 (1H, m), 7.23–7.39 (9H, m); δ_C [Major isomer] 17.8, 17.9, 36.2, 48.7, 52.5, 52.5, 56.9, 117.1, 124.1, 126.6, 128.6, 128.6, 129.0, 129.1, 131.9, 131.9, 132.8, 133.9, 137.1, 166.2, 170.9, 179.2. [Minor isomer] 17.8, 17.9, 36.1, 48.9, 52.3, 52.5, 56.9, 117.0, 124.1, 126.6, 128.3, 128.5, 129.0, 129.0, 131.8, 131.9, 132.9, 133.9, 137.1, 166.1, 170.9, 172.3; calcd for $C_{22}H_{26}N_4O_3 + H^+$ 395.2083 found 295.2085.

3.3.6. 6-(4-Hydroxy-benzyl)-9-(phenyl-phenylamino-methyl)-[1,4,7]triazecane-2,5,8-trione (6)

Yield 70%; off-white semi-solid; was isolated as inseparable mixture of diastereomer; γ_{max} (KBr/cm^{-1}) 1646, 1742, 2368, 3435. δ_H 2.97–3.17 (4H, m), 3.73–3.82 (3H, m), 5.16 (1H, d, J = 5.2 Hz), 5.22–5.27 (1H, m), 6.40 (1H, br s), 6.51 (1H, br s), 6.78–7.36 (14H, m). δ_C [Major isomer] 29.6, 36.0, 36.9, 52.5, 54.5, 57.0, 110.7, 115.6, 117.1, 124.2, 125.9, 126.6, 127.7, 128.5, 128.6, 128.8, 129.0, 130.3, 132.0, 133.7, 137.0, 143.5, 155.3, 166.3,

171.1; [Minor isomer] 29.2, 36.2, 37.2, 52.5, 54.5, 57.0, 110.7, 115.6, 117.1, 124.2, 125.9, 126.6, 127.7, 128.5, 128.6, 128.8, 129.0, 130.3, 132.0, 133.7, 137.0, 143.5, 155.3, 166.3, 171.1; HRMS calcd for $C_{27}H_{28}N_4O_4 + H^+$ 473.2190 found 473.2195.

3.3.7. 3,6,9-Trimethyl-12-(phenyl-phenylamino-methyl)-1,4,7,10 tetraaza-cyclotridecane-2,5,8,11-tetraone (7)

Yield 75%; off-white semi-solid; isolated as inseparable mixture of diastereomer; γ_{max} (KBr/cm^{-1}) 1644, 1748, 2345, 3428; δ_H 1.24–1.30 (9H, m), 2.95–3.27 (3H, m), 3.82 (1H, m), 4.34–4.37 (2H, m), 5.22 (1H, dd, $J1 = J2 = 5.6$ Hz), 6.63 (1H, br s), 6.83 (1H, br s), 7.04 (1H, m), 7.24–7.33 (9H, m), 7.80 (1H, br s). δ_C [Major isomer] 17.6, 17.7, 17.7, 36.0, 48.8, 49.0, 50.6, 52. 5, 57.0, 117.1, 124.1, 126.6, 126.6, 128.4, 128.5, 128.9, 129.0, 129.0, 133.8, 133.8, 137.1, 166.1, 172.1, 172.6, 176.4; [Minor isomer] 17.6, 17.7, 17.7, 36.2, 48.8, 48.9, 49.0, 52.3, 57.0, 117.1, 124.1, 126.6, 126.6, 128.4, 128.5, 128.9, 129.0, 129.1, 133.8, 133.8, 137.1, 166.2, 166.3, 172.3, 172.6; HRMS calcd for $C_{25}H_{31}N_5O_4 + H^+$ 466.2454 found 466.2458.

Acknowledgements

K.C. and D.D. thank Council of Scientific and Industrial Research (CSIR) and Department of Biotechnology (DBT), Government of India, respectively for fellowship. Central Research Facility and Department of Chemistry, IIT Kharagpur are thanked for providing all the instrumental facilities. A.B. and A.K.D. gratefully acknowledge the support of DBT for providing the necessary research grant.

Supplementary data

Supplementary data associated with this article can be found, in the online version, at doi:10.1016/j.bmc.2010.09.052.

References and notes

1. (a) Kennelly, P. J. In *Introduction to Cellular Signal Transduction*; Sitaramayya, A., Ed.; Birkhauser: Boston, 1999; pp 235–263; (b) Marks, F. In *Protein Phosphorylation*; Marks, F., Ed.; VCH Publisher: New York, 1996; pp 1–35; (c) Fischer, E. H.; Charbonneau, H.; Tonks, N. K. *Science* **1991**, *253*, 401; (d) Hunter, T. *Cell* **1995**, *80*, 225; (e) Bruke, T. R.; Zhang, Z. Y. *Biopolymers* **1998**, *47*, 225; (f) Baily, H.; Waldmann, H. *Angew. Chem., Int. Ed.* **2005**, *44*, 3814; (g) Moller, N. P.; Andersen, H. S.; Jeppesen, C. B.; Iversen, L. F. *HEP* **2005**, *167*, 215.
2. (a) Koul, A.; Choidas, A.; Treder, M.; Tyagi, A. K.; Drlica, K.; Singh, Y.; Ullrich, A. *J. Bacteriol.* **2000**, *182*, 5425; (b) Cowley, S. C.; Babakaiff, R.; Av-gay, Y. *Res. Microbiol.* **2002**, *153*, 233.
3. Cole, S. T.; Brosch, R.; Parkhill, J.; Garnier, T.; Churcher, C.; Harris, D.; Gordon, S. V.; Eiglmeier, K.; Gas, S.; Barry, C. E.; Tekaia, F.; Badcock, K.; Basham, D.; Brown, D.; Chillingworth, T.; Connor, R.; Davies, R.; Devlin, K.; Feltwell, T.; Gentles, S.; Hamlin, N.; Holroyd, S.; Hornsby, T.; Jagels, K.; Krogh, A.; McLean, J.; Moule, S.; Murphy, I.; Oliver, K.; Osborne, J.; Quail, M. A.; Rajandream, M. A.; Roger, J.; Rutter, S.; Seeger, K.; Skelton, J.; Squares, R.; Squares, S.; Sulston, J. E.; Taylor, K.; Whitehead, S.; Barell, B. G. *Nature* **1998**, *393*, 537.
4. (a) Castandt, J.; Prost, J.-F.; Peyron, P.; Dequeker, C. A.; Anes, E.; Cozzone, A. J.; Griffiths, G.; Parini, I. M. *Res. Microbiol.* **2005**, *156*, 1005; (b) Bach, H.; Sun, J.; Hmama, Z.; Av-Gay, Y. *Infect. Immun.* **2006**, *74*, 6540.
5. Madhurantakam, C.; Rajakumara, E.; Mazumdar, P. A.; Saha, B.; Mitra, D.; Wiker, H. G.; Sankaranarayanan, R.; Das, A. K. *J. Bacteriol.* **2005**, *187*, 2175.
6. (a) Barford, D.; Flint, A. J.; Tonks, N. K. *Science* **1994**, *263*, 1397; (b) Pannifer, A. D. B.; Flint, A. J.; Tonks, N. K.; Barford, D. *J. Biol. Chem.* **1998**, *273*, 10454.
7. (a) Manger, M.; Scheck, M.; Prinz, H.; Von Kries, K. P.; Langer, T.; Saxena, K.; Schwalbe, H.; Fuerstner, A.; Rademann, J.; Waldmann, H. *ChemBioChem* **2005**, *6*, 1749; (b) Bughin, C.; Masson, G.; Zhu, J. *J. Org. Chem.* **2007**, *72*, 1826.
8. (a) Pal, R.; Ghosh, S. C.; Chandra, K.; Basak, A. *Synlett* **2007**, 2321; (b) Alcaide, B.; Almendros, P. *Chem. Soc. Rev.* **2001**, *30*, 226; (c) Palomo, C.; Aizpurua, J. M.; Gamboa, I.; Oiarbide, M. *Curr. Med. Chem.* **2004**, *11*, 1837; (d)*Chemistry and Biology of β-Lactam Antibiotics*; Morin, R. B., Gorman, M., Eds.; Academic Press: New York, 1982; Vols. 1–3, (e) Banff, L.; Basso, A.; Guanti, G. *Tetrahedron* **1997**, *53*, 3249.
9. (a) Basak, A.; Chandra, K.; Pal, R.; Ghosh, S. C. *Synlett* **2007**, 1585; (b) Kinugasa, M.; Hasimoto, S. *Chem. Commun.* **1972**, 466.
10. (a) Banfi, L.; Guanti, G.; Rasparini, M. *Tetrahedron Lett.* **1998**, *39*, 9539; (b) Banfi, L.; Guanti, O. *Angew. Chem., Int. Ed. Engl.* **1995**, *34*, 2393; (c) Banff, L.; Guanti, G. *Eur. J. Org. Chem.* **1998**, 1543; (d) Tsang, W. Y.; Ahmed, M.; Page, M. I. *Org. Bio. Chem.* **2007**, *5*, 485.
11. (a) Kessler, H. *Angew. Chem., Int. Ed. Engl.* **1982**, *21*, 512; (b) Gung, B. W.; MacKay, J. A.; Zou, D. *J. Org. Chem.* **1999**, *64*, 700; (c) Litmas, M.; Klein, M. P. *J. Am. Chem. Soc.* **1975**, *97*, 4731.
12. Madhurantakam, C.; Chavali, V. R. M.; Das, A. K. *Proteins* **2007**, 706.
13. Whitmore, L.; Wallace, B. A. *Nucleic Acids Res.* **2004**, *32*, 668.
14. (a) Neault, J. F.; Ragi, C.; Novetta-Dellen, A.; Tajmir-Riahi, H. A. *Cell Biochem. Biophys.* **2006**, *46*, 27; (b) Whitmore, L.; Wallace, B. A. *Biopolymers* **2007**, *89*, 392.
15. (a) Lakowicz, J. R. *Principles of Fluorescence Spectroscopy*; Plenum Press: New York, 1983; (b) Lunardi, C. N.; Bonilha, J. B. S.; Tedesco, A. C. *J. Lumin.* **2002**, *99*, 61; (c) Eftink, M. R.; Ghiron, C. A. *J. Phys. Chem.* **1976**, *80*, 486; (d) Blart, E.; Chatelier, R. C.; Sawyer, W. H. *Biophysics* **1986**, 349; (e) Cao, H.; Liu, Q.; Shi, J.; Xiao, J.; Xu, M. *Anal. Lett.* **2008**, *41*, 521; (f) Mitra, D.; Mukherjee, S.; Das, A. K. *FEBS Lett.* **2006**, 6846.
16. (a) Moller, M.; Denicola, A. *Biochem. Mol. Biol. Ed.* **2002**, *30*, 309; (b) Cui, F.; Qin, L.; Zhang, G.; Liu, Q.; Yao, X.; Lei, B. *J. Pharm. Biomed. Anal.* **2008**, *48*, 1029; (c) Liu, J.; Tian, J.; He, W.; Xie, J.; Hu, Z.; Chen, X. *J. Pharm. Biomed. Anal.* **2004**, *35*, 671.
17. Lang, P. T.; Brozell, S. R.; Mukherjee, S.; Pettersen, E. T.; Meng, E. C.; Thomas, V.; Rizzo, R. C.; Case, D. A.; James, T. L.; Kuntz, I. D. *RNA* **2009**, *15*, 1219.
18. Pettersen, E. F.; Goddard, T. D.; Huang, C. C.; Couch, G. S.; Greenblatt, D. M.; Meng, E. C.; Ferrin, T. E. *J. Comput. Chem.* **2004**, *13*, 1605.